

## **Articles**

https://doi.org/10.20884/1.jm.2024.19.2.9964

### Fluorescent Turn-off Probe of Ni<sup>2+</sup> Based Nitrogen-Doped Carbon Dots

Siti Raudhatul Kamali<sup>1\*</sup>, Chang-Nan Chen<sup>2</sup>, Dinesh Chandra Agrawal<sup>2</sup>, Tai-Huei Wei<sup>3</sup>

<sup>1</sup>Department of Environmental Science, University of Mataram, Mataram, 83125, Indonesia <sup>2</sup>Department of Applied Chemistry, Chaoyang University of Technology, Taichung, 413310, Taiwan <sup>3</sup>Department of Physics, National Chung Cheng University, Chiayi, 621301, Taiwan

\*Corresponding author email: sitikamali@unram.ac.id

Received November 16, 2023; Accepted April 16, 2024; Available online July 20, 2024

**ABSTRACT:** An effective and facile method of generating nitrogen-doped carbon dots (N-CD) by microwave irradiation is presented in this study. A precursor, succinic acid (SA), and a nitrogen source, bis-(3-aminopropyl)-amine (BAPA), were used to obtain N-CD. A precious quantum yield (QY) of 49.0% was obtained from the preparation of N-CD, which was well-soluble in water. The N-CD material was highly selective and sensitive for the detection of nickel ion (Ni<sup>2+</sup>), with a detection limit of 0.26  $\mu$ M and a linear concentration range of 5-175  $\mu$ M. The quenching of the N-CD by the presence of Ni<sup>2+</sup> was referred to formation of complexes because of the interaction of Ni<sup>2+</sup> on the N-CD. Hence, the proposed study has great promise regarding Ni<sup>2+</sup> detection in broad applications.

**Keywords**: Microwave, Ni<sup>2+</sup>, nitrogen-doped carbon dots.

#### INTRODUCTION

Currently, the use of nickel (Ni) is widespread in a variety of fields as a result of its abundance, mainly for catalysts in the food industry, processes metallurgies, and the production of batteries (Chakraborty & Rayalu, 2015; Mudd, 2010). Although Ni is among the most widely used transition metals in the world, several facts indicate that Ni can be toxic to biological systems (Genchi et al., 2020). Furthermore, direct exposure to Ni would possibly cause undesirable effects on human health like lung cancer, respiratory system, and kidney cancer, and can badly increase blood cells (Dudek-Adamska et al., 2021). Drinking water and food consumption are the main contributors to Ni accumulation in the human body affecting the health of humans. Consumption of drinking water resulted in a relatively high absorption of Ni (25-27%) compared to food (0.7-2.5%) (Schrenk et al., 2020). In accordance with the WHO (2000), drinking water has been set at a maximum permissible limit (MCL) of 0.02 mg L-1 for the amount of Ni2+ (Pimsin et al., 2021). Because of that, detection and monitoring of nickel pollution levels in waters, which is an important part of daily human survival, is very crucial.

It has been discovered that several methods can be used to detect Ni<sup>2+</sup> ions in samples of chemical and biological materials. The common methods are FAAS (Karimi & Kafi, 2015), GFAAS (Han et al. 2018), HPLC (Rekhi et al., 2016), and ICP-MS (Quarles et al., 2014). There have been promising results obtained with all of the methods above, but there are some

limitations in the use of environmental samples due to the slow speed, high cost, and complicated operation required for the methods. Thus, finding an appropriate and good method that is capable of detecting Ni<sup>2+</sup> ions successfully is one of the most important recommendations.

Organic molecule fluorescent methods have been widely developed to overcome these shortcomings, but require methods chromophore compounds which are relatively difficult to prepare due to the complexity of synthesis processes. Therefore, probes that are quickly and easily synthesized with good specificity and accuracy are needed for Ni<sup>2+</sup> detection. Recently, researchers have been paying a great deal of attention to carbon dots (CDs) because of their excellent properties such as great chemical stability, high solubility in water, easy and safe synthesis route, intensely bright fluorescence, strong resistance to photobleaching, low toxicity, and widely used for ion and small molecule detections, as well as other fields (Ding et al., 2014; Kaczmarek et al., 2021; Kong et al., 2017). In addition, the intrinsic benefits of electron-rich CDs render them highly appropriate for the detection of particular compounds, such as metal ions. Several CDs made from different substances have been employed for a variety of purposes, including the detection of metal ions in water. Fluorescent CDs nanocomposites have more practical applications, are convenient, stable over time, and rapidly detection for mercury ions in water samples (Wang et al., 2023; Yin et al., 2023). For the

quick identification of trace Fe(III) ions in water, the silica compound-modified CDs demonstrated exceptional photoluminescence characteristics and fluorescence switch performance (Chen et al., 2023; Li et al., 2023). Even though CDs have many advantages and are increasingly being used in ion detection methods, only a handful of studies have reported that CDs can detect  $Ni^{2+}$  ions selectively.

The work presented here involved the fabrication of a new fluorescence method of N-CD for Ni<sup>2+</sup> detection via a one-step microwave irradiation technique through implementing succinic acid (SA) as carbon source and bis-(3-aminopropyl)-amine (BAPA) as nitrogen dopant. SA, a promising bio-based platform chemical, serves as a starting material for industrial chemicals and a feedstock biodegradable polybutylene succinate production (Chen et al., 2023). A four-carbon dicarboxylic acid known as succinic acid (SA) has the potential to serve as a precursor for the synthesis of heteroatom-doped carbon dots (Chae et al., 2017; Prathumsuwan et al., 2018). When CDs were first synthesized using only SA, they had no fluorescence and were poorly distributed in polar solvents such as water. Therefore, it becomes important to develop CDs with good quantum yield and dispersion in polar liquids.

A simple method to achieve this was to combine it with a functional group such as BAPA which contains three amine groups in its molecular structure. Modification of original CDs with amino groups had been successfully carried out using electrochemical techniques which resulted in the production of red, green, and blue luminescence as fluorescent probes (Zhao et al., 2022). Due to its similar atomic size to carbon and the fact that each nitrogen atom has five valence electrons, nitrogen is frequently employed as a doping in the creation of doped CDs. By introducing electrons created by nitrogen atoms in nanostructure, CDs' internal electronic environment can be changed, enhancing their fluorescence characteristics (Redondo-Fernandez et al., 2023). The electron cloud density of CDs will rise with nitrogen doping, adjusting its electron energy levels and raising the quantum yield. In addition, n-type or p-type carrier features can be produced by adjusting the CD's electrical structure (Yao et al., 2019; Yoo et al, 2019). Furthermore, heteroatom doping techniques and surface passivation which typically involves functional groups like amine and hydroxyl groups are elements that can enhance the quantum yield, fluorescence characteristics, and other physicochemical attributes of CDs. These intriguing qualities have spurred the development of new sensing and other application capabilities (Omar et al., 2022; Redondo-Fernandez et al, 2023; Xu et al., 2021). By combining SA with BAPA, it was expected that N-CD would be able to achieve better detection limits and detection ranges when applied to Ni<sup>2+</sup> detection applications. The performance of N-CD to detect Ni<sup>2+</sup> was investigated through a series of tests. Furthermore, good results were shown by the probe when applied to real water samples.

## EXPERIMENTAL SECTION

#### Chemicals

During the entire experiment, analytical grade chemicals were used for all of the chemicals.  $C_{40}H_{52}N_4O_9S$ ,  $HN[(CH_2)_3NH_2]_2$ ,  $C_4H_6O_4$ , RbCl,  $HgCl_2$ , and CsCl were purchased from Sigma-Aldrich (USA).  $Cr(NO_3).9H_2O$  was obtained from Alfa Aesar (USA).  $Mg(NO_3)_2.6H_2O$  and  $NiCl_2.6H_2O$  were purchased from Showa (Japan).  $MnSO_4.H_2O$  was procured from PanReac AppliChem (Germany) as well as  $CuSO_4.5H_2O$  was obtained from Choneye pure chemicals.

#### **N-CD Synthesis**

The strategy for utilizing microwave irradiation to create N-CD was developed based on prior methods (Kamali et al., 2021). This study was performed by dispersing 0.50 g of SA in 15.0 mL of deionized water (DI water), along with 1 mL of BAPA. The mixed solution was heated in the microwave for five minutes at 700 watts, then naturally cooled with the air. Following the complete dissolving of the product in 10 mL of DI water, centrifugation at 10.000 rpm was conducted on the resulting solution. In the next step, a cylinder membrane filter (0.22  $\mu$ m) was used to filter the clear solution, which was then purified with dialysis. The purified solution was finalized by freezedrying and kept at 4  $^{0}$ C, so that further testing could be conducted.

#### Characterization

N-CD morphology and size were examined under transmission electron microscopy (TEM) JEOL JEM-2010 (Japan) with an accelerating voltage of 200 kV. To confirm the functional group of the N-CD surface, a Fourier transform infrared (FTIR) spectrometer, Perkin Elmer (USA) was used. On the other hand, the elemental analysis of N-CD was investigated using X-ray photoelectron spectroscopy (XPS) on a PHI Hybrid Quantera. An FP-750 fluorescence spectrophotometer, Jasco (Japan) was conducted to measure N-CD photoluminescence (PL) intensity. Absorption spectra were measured by a Lambda 265 ultraviolet-visible (UV-Vis) spectrophotometer, Perkin Elmer (USA).

#### Measurement of QY

The QY calculation of N-CD refers to the QY equation based on equation (1).

$$QY_{n} = QY_{r} \frac{I_{n} A_{r} \eta_{n}^{2}}{I_{r} A_{n} \eta_{r}^{2}}$$
 (1)

Where subscripts "n" and "r" refer to N-CD and quinine sulfate, respectively. While "I," "A," and " $\eta$ " correspond to the PL intensity, the measured absorbance at the selected excited wavelength, and the solvent refractive index, respectively. Quinine sulfate was preferred as the standard due to its stable luminescent properties.

Furthermore, the PL emission measurement was conducted at the 370 nm excitation wavelength.

#### Stability tests

As part of evaluating the effect of chloride ion concentrations, different concentrations of sodium chloride were added to 10  $\mu$ L of N-CD ranging from 0 to 200 mM. A further stability test was performed by conditioning the N-CD solution at various pH levels from 1 to 13. In order to vary the pH of the N-CD solution, various solutions of HCl or NaOH were added. Using a UV-irradiation lamp (365 nm) to irradiate N-CD for two hours with intervals of 10 minutes was used to assess the photostability of N-CD. As a final step, a number of different temperatures were applied, including 25 °C, 35 °C, 45 °C, 55 °C, 65 °C, and 75 °C. After that, the intensity of the PL was recorded for each stability test that was conducted.

#### Sensitivity and selectivity of Ni<sup>2+</sup>

In order to estimate the selectivity of the N-CD solution, a specific amount of N-CD solution (0.01 mg/mL) was tested with a specific amount of several ions. These ions were Ni<sup>2+</sup>, Cs<sup>+</sup>, K<sup>+</sup>, Li<sup>+</sup>, Mn<sup>2+</sup>, Na<sup>+</sup>, Rb<sup>+</sup>, Hg<sup>2+</sup>, Cr<sup>3+</sup>, Pb<sup>2+</sup>, Ag<sup>+</sup>, Mg<sup>2+</sup>, Zn<sup>2+</sup>, CO<sub>3</sub><sup>2-</sup>, PO<sub>4</sub><sup>3-</sup>, Cu<sup>2+</sup>, and Fe<sup>2+</sup> with an ionic concentration of 200 mM for each of ion in the solution. Moreover, a wide range of concentrations of Ni<sup>2+</sup> was used in the evaluation of the sensitivity and concentration range of Ni<sup>2+</sup> ion, ranging from 0 – 200  $\mu$ M. Each solution was mixed thoroughly after the addition of Ni<sup>2+</sup> and DI water. The solution was allowed to react for 5 min, and the PL spectrum was measured at 370 nm, which corresponds to the excitation wavelength.

# RESULTS AND DISCUSSIONS N-CD synthesis

N-CD was synthesized by a microwave irradiation process with SA functioning as a precursor and BAPA serving as a source of nitrogen. There were a number of combinations of doping amount, microwave power, and irradiation time that were tested in order to obtain the best conditions for synthesizing N-CD with the highest QY as shown in **Table 1**.

The blue color solution under UV lamp 365 nm produced by SA-BAPA subjected to 700 W microwave radiation for five minutes indicated the abundance of functional groups, which leads to an increase in the number of fluorescent CDs and improvement in QY (Hayden et al., 2023; Ghanem et al., 2020). In light of this, it appears that N-CDs that have a high degree of QY using a BAPA solution 1 mL, A volume of BAPA that corresponds to the amount of precursor and appropriate reaction conditions can promote the formation of CDs with a higher level of uniformity (Shibata et al., 2022). In the meantime, the quantity of BAPA, which was 0.5 milliliters, combined with a shorter irradiation duration and lower microwave irradiation, was not sufficient to achieve complete carbonization. After that, the strength of the photoluminescence was altered, and it showed up to

be less powerful than it had been previously (Ang et al. 2021).

Thus, the optimum condition for producing the highest QY of N-CD was 1 mL of BAPA, 700 W of microwave power, and 5 minutes of irradiation time. Therefore, these conditions were set for further experiments. The quantum yield produced under the optimum condition was 49.00%, meaning that in 100 units of energy (photons) passing through the solution, an amount of 49.00 was emitted in the form of fluorescence emission. The lowest quantum yield was 11.18% at 0.5 mL of BAPA, 500 W of microwave power, and 4 minutes of irradiation time.

#### Characterization of N-CD

N-CD was measured by TEM in terms of size and morphology. Based on the TEM image shown in Figure 1a, a fairly consistent size distribution was observed for the N-CD particles, which were almost dispersed spherical particles, with a size distribution of about 27 nm. Particle sizes over 10 nm have primarily been ascribed to the phenomenon of agglomeration Varisco et al., 2017. The tendency for carbon dots to cluster in the solid state is related to their small size, resulting in a rise in the average diameter (Hagiwara et al., 2020; Liu et al., 2017). The FTIR spectra provided a detailed insight into the surface functional groups of the synthesized N-CD. According to Figure 1b, the characteristic peaks at the frequencies of 632, 1261, 1554, 3264, and 3431 cm<sup>-1</sup> as being associated with the stretches of the C-H, C-N, C=C, N-H, and O-H vibrations. These peaks are related to hydroxyl groups and amide groups on N-CD (Zhang et al., 2018; Yanyan et al., 2021; Lin et al., 2019; Sadhanala et al., 2022). At 2939 cm<sup>-1</sup>, vibrations of C-H hydrogen bonds indicated the presence of saturated hydrocarbons (Fan et al., 2018), and the carbonyl group (C-O) was detected at 1118 cm-1 (Chang et al., 2022). There was an additional peak at 1639 cm<sup>-1</sup> which was associated with the stretching vibration of the C=O group, indicating that carboxylic groups were present on the N-CD (Issa et al., 2019; Wang et al., 2020).

An XPS spectrum, observing the chemical composition of the surface of the N-CD and their elemental composition was displayed in Figure 2a. It was found that 69.8% of the N-CD synthesized was composed of carbon, followed by 13.2% of nitrogen, and 17.0% of oxygen. In terms of the strong peaks, there were three typical peaks linked to C1s, N1s, and O1s. As a result of deconvolving the high-resolution spectrum of C1s, four peaks can be discerned at 284.8, 285.8, 286.4, and 287.6 eV, these being the peaks of the C=C, C-C, C-N, and C-O bonds, respectively (Figure 2b-d). Deconvolution of the high-resolution Ols spectrum resulted in two prominent peaks in the spectrum at 531.2 and 532.4 eV, which correspond with the characteristics of the C=O and C-O (Wang et al., 2020). In the XPS spectrum of N1s at high

resolution, two peaks were found at 400.8 eV and 399.0 eV, which correspond to C–N and N–H (Chang et al., 2022; Basoglu et al., 2020). There was a good agreement between the XPS data and the FTIR data obtained. A study on the N-CD synthesized indicated that there were functional groups containing oxygen and nitrogen like –COOH, -NH, and -OH (Arul & Sethuraman, 2019; Liu et al., 2019;

Sun et al., 2022). In N-CD, these three functional groups constitute the most commonly found ligands that can be introduced either covalently or noncovalently (Domingo-Tafalla et al., 2022). Furthermore, the presence of functional groups implies that the N-CD could be used for a number of additional purposes due to their excellent solubility in water (Liu et al., 2019).

**Table 1**. Quantum yield of N-CD synthesis at different BAPA volumes, microwave powers, and irradiation times

| No. | Volume of BAPA<br>(ml) | Irradiation time<br>(min) | Microwave power (watt) | Quantum yield<br>(%) |
|-----|------------------------|---------------------------|------------------------|----------------------|
| -   |                        | (111111)                  | \ /                    |                      |
| 1   | 0.5                    | 4                         | 500                    | 17.18                |
| 2   | 1.0                    | 4                         | 500                    | 33.48                |
| 3   | 0.5                    | 5                         | 500                    | 28.39                |
| 4   | 1.0                    | 5                         | 500                    | 45.28                |
| 5   | 0.5                    | 4                         | 700                    | 28.99                |
| 6   | 1.0                    | 4                         | 700                    | 33.84                |
| 7   | 0.5                    | 5                         | 700                    | 21.44                |
| 8   | 1.0                    | 5                         | 700                    | 49.00                |

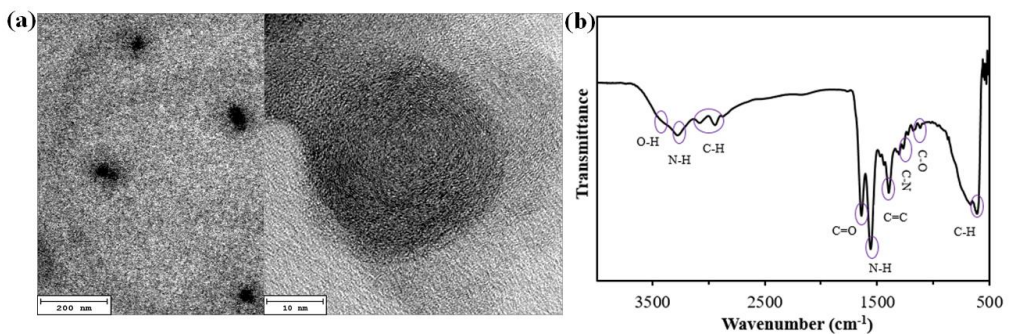


Figure 1. (a) Image profile of N-CD captured using TEM and (b) N-CD FTIR spectrum

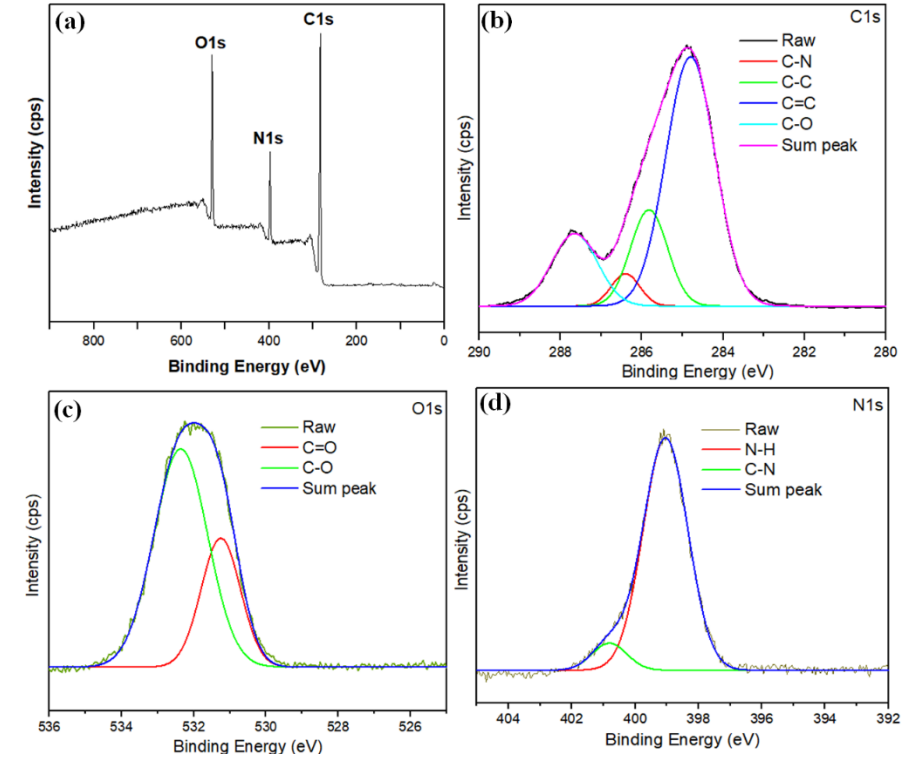
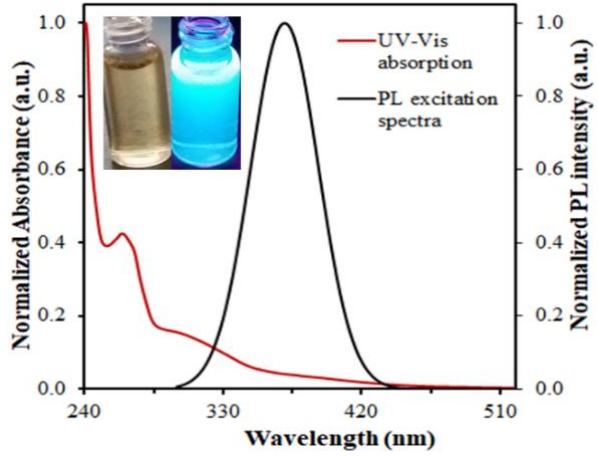


Figure 2. (a) N-CD survey spectra, XPS spectra of (b) C1s, (c) O1s, and (d) N1s

#### **N-CD Optical Properties**

The blue luminescence of the N-CD solution under UV light 365 nm was an early indication of successful of N-CD synthesis (inset **Figure 3**). The N-CD was also investigated using UV-Vis and PL spectra to determine its optical properties. Based on the N-CD absorption spectrum in **Figure 3**, a prominent peak was observed at 270 nm, which was associated with a  $\pi - \pi^*$  transition of C=C or C=N (Ding et al., 2014; Jayaweera et al., 2019). The shoulder peak could be observed at 298 nm, corresponding to  $n - \pi^*$ , which could be ascribed to transition by the functional group of oxygen or nitrogen on the N-CD surface (Nemati et al., 2018; Ghanem et al., 2020; Dsouza et al., 2021). The N-CD also exhibited wavelength-dependent fluorescence emissions. Based on the

different excitation wavelengths, two fluorescence emission regions were found. A red shift in the fluorescence emission can be observed as a result of the excitation of fluorescence between 300 and 340 nm and 350 and 500 nm. It was then found that the highest value of the fluorescence emission of 459 nm had been observed at the wavelenath of excitation of 370 nm. Aside from these observations, the lowest emission was found at the wavelength of 500 nm, and the fluorescence was absent at excited fluorescence over 500 nm. The dependence of the resulting N-CD emission at different N-CD excitation wavelengths could be attributed to the carbon core size distribution nonuniformity and the presence of multiple surface sites on the N-CD (Lin et al., 2019).



**Figure 3**. Inset photos of N-CD (left: daylight, right: UV light, 365 nm) with spectra (red line: UV-Vis absorption, black line: PL excitation).

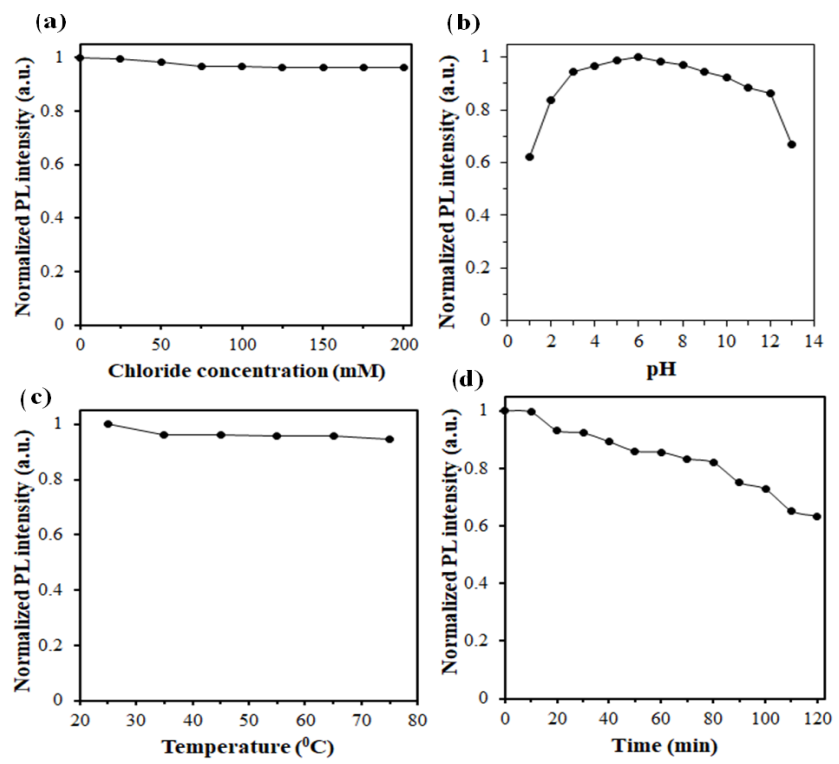


**Figure 4**. Stability of N-CD at (**a**) different chloride concentrations, (**b**) different pH levels, (**c**) different temperatures, and (**d**) Irradiation 365 nm UV light

When the atoms of C and N are combined, there is a tendency between the atoms of C and N to form strong bonds when they are in contact with each other. The existence of electron pairs and defect sites that usually appear would also provide the possibility of active sites and modifying the chemical activity of CDs (Niu et al., 2014). N-CD could commonly exist as graphitic-N, pyrrolic-N, and/or pyridinic-N by substituting C in the center or at the edges of the structure with N. In addition, elemental N would modify the N-CD optical properties by changing the edges of the bandgap or creating new energy levels to increase fluorescence and to produce the number of photons emitted for a particular application (Lin et al., 2019; Dejpasand et al., 2020). In the case of N-CD, BAPA could react with carboxyl or epoxy groups which an important role in non-radiative recombination to enhance PL emission of N-CD (Rao et al., 2018). Various functional groups have the possible ability to supply electrons to N-CD, thus giving different energy levels.

To prove the N-CD synthesized could be applied fluorescence sensors under environmental conditions, the stability of PL of N-CD was considered essential to evaluate. Figure 4a illustrates that there appeared to be a consistent pattern in the PL intensity of the N-CD over a range of NaCl concentrations between 0 and 200 mM. Based on the results of the study, it was determined that the synthesized N-CD could be used at high salt concentrations due to its strong colloidal properties and its ability to resist the force of particle attraction (Kumari et al., 2022). Figure **4b** shows that the synthesized N-CD exhibited a wide pH response range from 1.0 to 13.0. The PL intensity exhibited a downward trend under highly acidic and basic conditions. A probable explanation for this phenomenon is that it might be connected to protonation and deprotonation processes that cause chemical changes on the surface of the N-CD (Al-Hashimi et al., 2020; Xu et al., 2022). A carboxyl group that can be protonated at the carbon dots synthesized in an acid solution (Almaquer et al., 2019). The maximum PL intensity was reached at 6, which might be ascribed to the many hydrophilic carboxyls on the N-CD surface. It has been found that the PL intensity in the pH ranges between 3 and 10

remains remarkably constant over time. Accordingly, this was consistent with the N,S-CDs synthesized by another researcher who also demonstrated similar pH characteristics (Xu et al., 2021), which also showed similar pH characteristics. **Figure 4c-d** shows that the increasing temperature decreases the intensity of PL. It appears that the reduction in PL intensity is due to the activation of non-radiative thermal traps. It was also found that the PL intensity of the N-CD was subject to changes when continuous UV irradiation was applied for 120 minutes. The synthesized N-CD exposed to UV radiation decreased the PL intensity by 14% after 60 min.

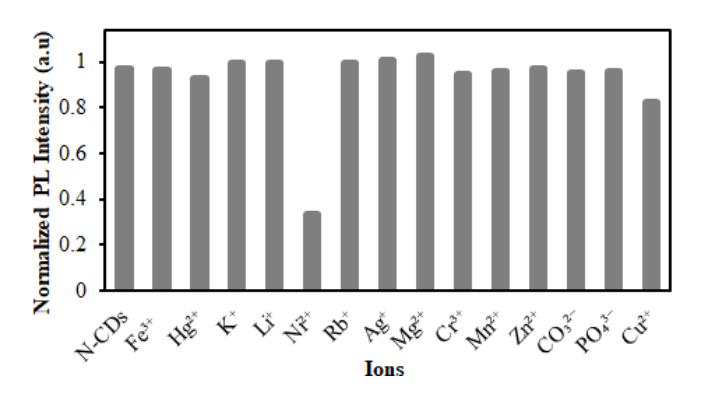
#### N-CD selectivity and sensitivity to Ni<sup>2+</sup>

In order to investigate the selectivity of the N-CD as the fluorescence sensor for Ni $^{2+}$ , the PL intensity of the synthesized N-CD was assayed with various ions at the same conditions and recorded at 370 nm as the wavelength of excitation. The metal ions were K+, Ni $^{2+}$ , Hg $^{2+}$ , Li<sup>+</sup>, Rb<sup>+</sup>, Ag<sup>+</sup>, Mg $^{2+}$ , Cr $^{3+}$ , Mn $^{2+}$ , Zn $^{2+}$ , Fe $^{3+}$ , CO $_3^{2-}$ , PO $_4^{3-}$ , and Cu $^{2+}$  with each concentration of 200  $\mu$ M. By comparing the intensity ratio of PL of N-CD solution with the existence of heavy metal ions (**Figure 5**), it was found that Ni $^{2+}$  possibly quenched the N-CD fluorescence. The quenching efficiency of Ni $^{2+}$  reached 60% among the other ions. Therefore, N-CD could be used to detect Ni $^{2+}$  selectively.

**Figure 6a** shows that Ni<sup>2+</sup> can quench the N-CD intensity. By increasing Ni<sup>2+</sup> concentration, the N-CD PL intensity of N-CD decreased significantly. However, the fluorescence wavelength was not affected. In addition, the PL intensity became very weak when the Ni<sup>2+</sup> concentration was 200  $\mu$ M. As shown in **Figure 6b**, a linear relationship was presented by the Stern-Volmer equation (2) (Xu et al., 2021).

$$\frac{F_0}{F} = 1 + Ksv + C \tag{2}$$

C represents Ni²+ concentration, whereas Ksv represents a quenching constant. In contrast,  $F_0$  and F refer to the PL intensity of N-CD with and without metal ions, respectively. Furthermore, based on the results of this study, a correlation coefficient of 0.995 was observed between the concentrations of 5-175  $\mu M$ . The detection limit (LOD) was obtained at 0.25  $\mu M$  according to  $3\delta/m$  (where  $\delta$  denotes the blank signal's standard deviation and m is the slope of the linear relationship, respectively) (Xu et al., 2022).



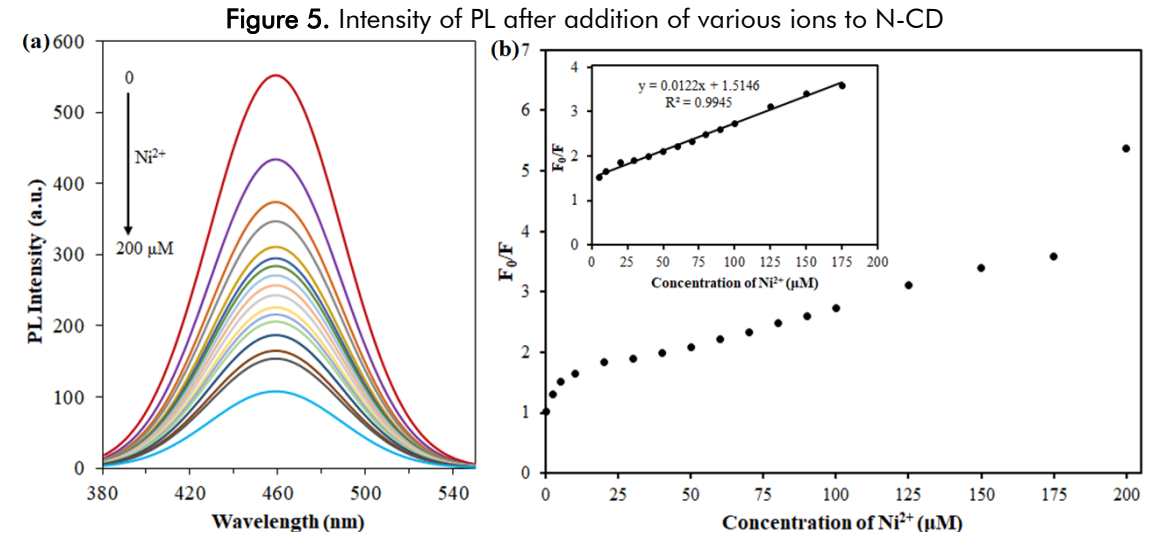


**Figure 6**. (a) PL emission spectra of various concentrations of Ni<sup>2+</sup>, (b) Curve of Stern-Volmer with an inset a linear curve for Ni<sup>2+</sup> (5-175  $\mu$ M)

**Table 2**. Review of the various methods for Ni<sup>2+</sup> detection

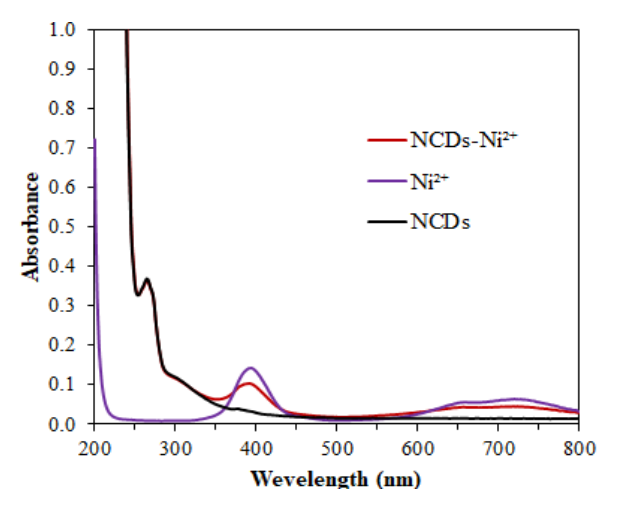
| Method                                  | Linear range              | LOD                    | Reference               |
|---|---------------------------|------------------------|-------------------------|
| Citrate-stabilized silver nanoparticles | 0.7-1.6 mM                | 0.75 mM                | (De Paula et al., 2019) |
| NGr-DMG modified GCE                    | 2-20 μg L <sup>-1</sup>   | 1.5 μg L <sup>-1</sup> | (Pokpas et al., 2017)   |
| CD-imidazole                            | 6-100 mM                  | 0.93 mM                | (Gong & Liang, 2019)    |
| DMG-N-GQDs                              | 50-200 μg L <sup>-1</sup> | 20 μg L <sup>-1</sup>  | (Pimsin et al., 2021)   |
| Boron nitride quantum dots (BNQDs)      | 0.1-100 μΜ                | 0.1 μΜ                 | (Yao et al., 2017)      |
| Nitrogen-doped carbon dots (N-CD)       | 5-175 μΜ                  | 0.25 μΜ                | This work               |

Based on the results presented in **Table 2**, the probe provided a lower detection limit (LOD) and a wider linear range compared with other probes that had been reported. In addition, its detection limit was found to be lower than that stated by WHO for a contaminant in drinking water, with a maximum limit allowed of 0.02 mg L<sup>-1</sup> as specified in its guidelines. As a result, this method has advantages over the other approaches, such as the simplicity of the synthesis of N-CD, the lower cost of raw materials, and the lower environmental impact.

#### Possible mechanism of quenching

To investigate the possible quenching mechanism, UV-visible spectroscopy of N-CD solutions with and

without nickel ions was used. Based on a comparison of the absorption spectrum of N-CD (black color and the absorption spectrum of N-CD interacted with Ni<sup>2+</sup> (red color) was shown in **Figure 7**. As can be seen in the figure, the strong absorption peaks of synthesized N-CD are 265 nm. There was an interesting observation in that the Ni<sup>2+</sup> absorption spectrum did not appear to have an absorption peak at 265 nm, but this peak was clearly visible when interacting with N-CD. Nevertheless, the wavelength of Ni<sup>2+</sup> absorption shifted to a shorter wavelength (390 nm) after interacting with N-CD and the intensity of Ni<sup>2+</sup> absorption in the 640-756 nm decreased after interacting with N-CD as well.



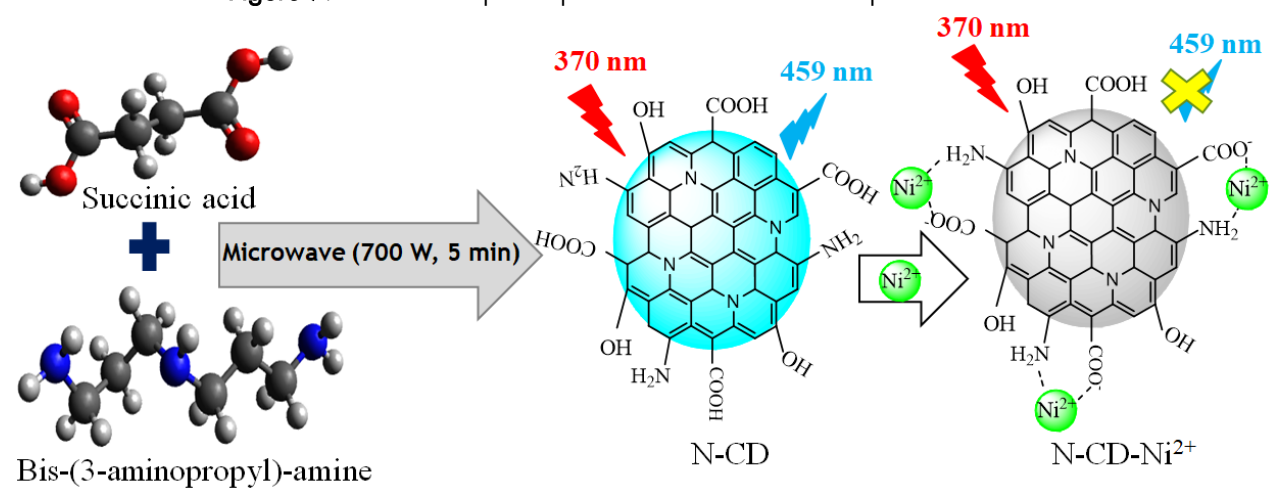


Figure 7. N-CD absorption spectra in the absence and presence of Ni<sup>2+</sup>

Figure 8. An illustration of fluorescent N-CD for the detection of Ni<sup>2+</sup>

There was nitrogen found on the surface of N-CD derived from amine groups present in the BAPA. Having the presence of electron donor nitrogen might lead to the donation of its electron pair to the electron acceptor Ni<sup>2+</sup>, thus resulting in the formation of the complex. Since part of the excitation light is absorbed by the N-CD-Ni<sup>2+</sup> complex, fewer excitation photons are available to excite the N-CD. This results in a reduction in the PL intensity emitted by the N-CD. In other words, the presence of Ni<sup>2+</sup> ions reduced the amount of light that can be emitted by the N-CD. The process of detecting Ni<sup>2+</sup> ions with N-CD can be seen in **Figure 8**.

#### **CONCLUSIONS**

In conclusion, microwave irradiation has successfully been used as a method of creating N-CD with a high quantum yield as well as having excellent water solubility. The mechanism can be harnessed for selective detection of  $Ni^{2+}$  ions because the fluorescence quenching is specific to the formation of the complex. By monitoring the decrease in PL intensity, the concentration of  $Ni^{2+}$  ions in a sample can be quantified, making it a valuable tool for analytical chemistry and trace metal ion detection, especially for  $Ni^{2+}$  ion detection.

#### **ACKNOWLEDGMENTS**

We acknowledge the support provided by Chaoyang University of Technology for our experiments. We are also thankful to all those who contributed to the successful completion of this research.

#### **REFERENCES**

Al-Hashimi B., Rahman H. S., & Omer K. M. (2020). Highly luminescent and biocompatible P and N Co-doped passivated carbon nanodots for the sensitive and selective determination of rifampicin using the inner filter effect. *Materials*,

*13*(10), 2275. https://doi.org/10.3390/ma 13102275

Almaquer F. E. P., Ricacho J. S. Y., & Ronquillo R. L. G. (2019). Simple and Rapid Colorimetric Sensing of Ni(II) ions in tap water based on aggregation of citrate-stabilized silver nanoparticles. *Sustainable Environment Research*, 29(1), 1-10. http://dx.doi.org/10.1186/s42834-019-0026-3

Ang W.L., Alqasem Q.A., & Mohammad A.W. (2021). Carbon dots from palm fronds biomass wastes. IOP Conf. Series: Materials Science and Engineering, 1195, 012008. https://doi.org/ 10.1088/1757-899X/1195/1/012008

Arul V., & Sethuraman M. G. (2019). Hydrothermally green synthesized nitrogen doped carbon dots from *Phyllanthus emblica* and their catalytic ability in the detoxification of textile effluents. *ACS Omega, 4*(2), 3449-3457. https://doi.org/10.1021/acsomega.8b03674

Başoğlu A., Ocak U., & Gümrükçüoğlu A. (2020). Synthesis of microwave-assisted fluorescence carbon quantum dots using roasted–chickpeas and its applications for sensitive and selective detection of Fe<sup>3+</sup> ions. *Journal of Fluorescence*, 30(3), 515–526. https://doi.org/10.1007/s10895-019-02428-7

Chae A., Choi Y., Jo S., Nur'aeni, Paoprasert P., Park S.Y., & In I. (2017). Microwave-assisted synthesis of fluorescent carbon quantum dots from an A<sub>2</sub>/B<sub>3</sub> monomer set. *RSC Advances*, 7(21), 12663-12669, https://doi.org/10.1039/C6RA28176A.

Chakraborty S., & Rayalu S. (2015). Detection of nickel by chemo and fluoro sensing technologies. Spectrochimica Acta, Part A: Molecular and Biomolecular Spectroscopy, 245, 118915. https://doi.org/10.1016/j.saa. 2020.118915

Chang K., Zhu Q., Qi L., Guo M., Gao W., & Gao Q. (2022). Synthesis and Properties of Nitrogen Doped Carbon Quantum Dots Using Lactic

- Acid As Carbon Source. *Materials*, *15*(2), 466. http://dx.doi.org/10.3390/ma15020466
- Chen T., Xu Y.T., Guo Q., Chen X., Su Q., & Cao Y. (2023). Oxytetracycline-Derived Carbon Dots As A Fluorescent Switch In Trace Ferric Ion Sensing. New Journal of Chemistry, 47, 11919–11927. https://doi.org/10.1039/D3NJ01930F
- Chen X., Wu H., Chen Y., Liao J., Zhang W., & Jiang M. (2023). Recent advancements and strategies of improving CO<sub>2</sub> utilization efficiency in biosuccinic acid production. *Fermentation*, 9(11), 967. https://doi.org/ 10.3390/fermentation 9110967.
- Dejpasand M. T., Saievar-iranizad E., Bayat A., Montaghemi A., & Ardekani S. R. (2020). Tuning HOMO and LUMO of three region (UV, Vis and IR) photoluminescent nitrogen doped graphene quantum dots for photodegradation of methylene blue. *Materials Reserach Bulletin*, 128, 110886. https://doi.org/10.1016/j.materresbull.2020.110886
- De Paula N. T. G., Milani R., Lavorante A. F., & Paim A. P. S. (2019). Use of carbon dots synthesized from citrate as a fluorescent probe for quercetin determination in tea and beer samples. *Journal of Brazilian Chemical Society*, 30(11), 2355–2366. http://dx.doi.org/10.21577/0103-5053.20190145
- Ding H., Wei J. S., & Xiong H. M. (2014). Nitrogen and suphur Co-doped carbon dots with strong blue luminescence. *Nanoscale*, 6(22), 13817-13823. https://doi.org/10.1039/C4NR04267K
- Domingo-Tafalla B., Martínez-Ferrero E., Franco F., & Palomares-Gil E. (2022). Applications of carbon dots for the photocatalytic and electrocatalytic reduction of CO<sub>2</sub>. *Molecules*, 27(3), 1081. https://doi.org/10.3390/molecules27031081
- Dsouza S. D., Buerkle M., Brunet P., Maddi C., Padmanaban B. D., Morelli A., Payam A. F., Maguire P., Mariotti D., & Svrcek V. (2021). The importance of surface states in N-doped carbon quantum dots. *Carbon*, 183, 1-11. https://doi.org/10.1016/j.carbon.2021.06.088
- Dudek-Adamska D., Lech T., Konopka T., & Kościelniak P. (2021). Nickel content in human internal organs. *Biological Trace Element Research*, 199, 2138-2144. https://doi.org/10.1007/s12011-020-02347-w
- Fan C., Ao K., Lv P., Dong J., Wang D., Cai Y., Wei Q., & Xu Y. (2018). Fluorescent nitrogen doped carbon dots via single-step synthesis applied as fluorescent probe for the detection of Fe<sup>3+</sup> ions and anti-counterfeiting inks. *Nano*, 13(8), 1850097. http://dx.doi.org/10.1142/S1793 292018500972
- Genchi G., Carocci A., Lauria G., Sinicropi M. S., & Catalano A. (2020). Nickel: Human health and

- environmental toxicology. *International Journal of Environmental Research and Public Health*, 17(3), 679. https://doi.org/10.3390%2 Fijerph 17030679
- Ghanem A., Al-Marjeh R.A.B., & Atassi Y. (2020). Novel nitrogen doped carbon dots prepared under microwave-irradiation for highly sensitive detection of mercury ions. *Heliyon*, **6**: e03750. https://doi.org/10.1016/j.heliyon.2020.e03750
- Gong Y., & Liang H. (2019). Nickel ion detection by imidazole modified carbon dots. Spectrochimica Acta Part A: Molecular and Biomolecular Spectroscopy, 211, 342-347. https://doi.org/10.1016/j.saa.2018.12.024
- Hagiwara K., Uchida H., Suzuki Y., Hayashita T., Torigoe K., Kida T., & Horikoshi S. (2020). Role of alkan-1-ol solvents in the synthesis of yellow luminescent carbon quantum dots (Cqds): Van der waals force-caused aggregation and agglomeration. *RSC Advances*, 10, 14396. http://dx.doi.org/10.1039/d0ra01349h
- Han Q., Huo Y., Yang L., Yang X., He Y., & Wu J., (2018). Determination of trace nickel in water samples by graphite furnace atomic absorption spectrometry. *Molecules*, 23(10), 2597. https://doi.org/10.3390/molecules231 02597
- Hayden, F. (2023). Carbon dot nanoparticles. *Theses Paper*, 803, https://dc.etsu.edu/honors/803.
- Issa M. A., Abidin Z. Z., Sobri S., Rashid S., Mahdi M. A., Ibrahim N. A., & Pudza M. Y. (2019). Facile Synthesis of nitrogen doped carbon dots from lignocellulosic waste. *Nanomaterials*, 9(10), 1500. https://doi.org/10.3390/nano9101500
- Jayaweera S., Yin K., & Ng W. J. (2019). Nitrogen doped durian shell derived carbon dots for inner filter effect mediated sensing of tetracycline and fluorescent ink. *Journal of Fluorescence*, 29(6), 221-229. https://link.springer.com/article/10.1007/ s10895-018-2331-3
- Kaczmarek A., Hoffman J., Morgiel J., Moʻscicki T., Stobiʻnski L., Szyma'nski Z., & Małolepszy A. (2021). Luminescent carbon dots synthesized by the laser ablation of graphite in polyethylenimine and ethylenediamine. *Materials*, 14(4), 729. https://doi.org/10.3390/ma14040729
- Kamali S.R., Chen C.N., Agrawal D.C., & Wei T.H. (2021). Sulfur-doped carbon dots synthesis under microwave irradiation as turn-of fuorescent sensor for Cr(III). *Journal of Analytical Science and Technology*, 12(1), 48. https://doi.org/10.1186/s40543-021-00298-y.
- Karimi M.A., & Kafi M. (2015). Removal, preconcentration and determination of Ni(II) from different environmental samples using modified magnetite nanoparticles prior to flame atomic absorption spectrometry. *Arabian*

- *Journal of Chem*istry, 8(6), 812-820. https://doi.org/10.1016/j.arabjc.2013.05.018
- Kong W., Wu D., Xia L., Chen X., Li G., Qiu N., Chen G., Sun Z., You J., & Wu Y. (2017). Carbon dots for fluorescent detection of α-glucosidase activity using enzyme activated inner filter effect and its application to anti-diabetic drug discovery. *Analytica Chimica Acta*, 973(2017), 91-99. https://doi.org/10.1016/j.aca.2017. 03.050
- Kumari M., Chaudhary G. R., Chaudhary S., Umar A., Akbar S., & Baskoutas S. (2022). Bio-derived fluorescent carbon dots: Synthesis, properties and applications. *Molecules*, 27(16), 5329. https://doi.org/10.3390/molecules27165329
- Li C., Xu X., Wang F., Zhao Y., Shi Y., Zhao X., & Liu J. 2023. Portable smartphone platform integrated with paper strip-assisted fluorescence sensor for ultrasensitive and visual quantitation of ascorbic acid. Food Chemistry, 402(14), 134222. https://doi.org/10.1016/j.foodchem.2022.134222
- Lin H., Huang J., & Ding L. (2019). Preparation of carbon dots with high-fluorescence quantum yield and their application in dopamine fluorescence probe and cellular imaging, *Journal of Nanomaterials*, 2019, 1-9. http://dx.doi.org/10.1155/2019/5037243
- Liu H., Zhao X., Wang F., Wang Y., Guo L., Mei J., Tian C., Yang X., & Zhao D. (2017). Highefficient excitation-independent blue luminescent carbon dots. Nanoscale Research Letters, 12, 399. http://dx.doi.org/10.1186/ s11671-017-2137-2
- Liu Y., Jiang L., Li B., Fan X., Wang W., Liu P., Xu S., & Luo X. (2019). Nitrogen doped carbon dots: mechanism investigation and their application for label free CA125 analysis. *Journal of Materials Chemistry B*, 7)19), 3053. https://doi.org/10.1039/C9TB00021F
- Liu W., Zhang R., Kang Y., Zhang X. Y., Wang H. J., Li L. H., Diao H. P., & Wei W. L. (2019). Preparation of nitrogen doped carbon dots with a high fluorescence quantum yield for the highly sensitive detection of Cu<sup>2+</sup> ions, drawing anticounterfeit patterns and imaging live cells. *New Carbon Mater*ials, 34(4), 390-402. https://doi.org/10.1016/S1872-5805 (19)300 24-1
- Mudd G. M. (2010). Global Trends and Environmental Issues in Nickel Mining: Sulfides Versus Laterites. *Ore Geology Reviews*, 38(1-2), 9-26. https://doi.org/10.1016/j.oregeorev. 2010.05.003
- Nemati F., Zare-Dorabei R., Hosseini M., & Ganjali M. R. (2018). Fluorescence turn-on sensing of thiamine based on arginine functionalized graphene quantum dots (Arg-GQDs): Central composite design for process optimization.

- Sensors and Actuators B: Chemical, 255(2), 2078-2085. https://doi.org/10.1016/j.snb. 2017.09.009
- Niu J., Gao H., Wang L., Xin S., Zhang G. Y., Wang Q., Guo L., Liu W., Gao X., & Wang Y. (2014). Facile synthesis and optical properties of nitrogen doped carbon dots. *New Journal of Chemistry*, 38(4), 1522–1527. https://doi.org/ 10.1039/C3NJ01068F
- Omar N.A.S., Fen Y.W., Irmawati R., Hashim H.S., Ramdzan N.S.M., & Fauzi N.I.M. (2022). A Review on carbon dots: Synthesis, characterization and its application in optical sensor for environmental monitoring. *Nanomaterials*, 12(14), 2365. https://doi.org/10.3390/nano12142365.
- Pimsin N., Kongsanan N., Keawprom C., Sricharoen P., Nuengmatcha P., Oh W. C., Areerob Y., Chanthai S., & Limchoowong N. (2021). Ultratrace detection of nickel(II) ions in water samples using dimethylglyoxime-doped GQDs as The Induced metal complex nanoparticles by a resonance light scattering sensor. ACS Omega, 6(23), 14796-14805. https://doi.org/10.1021/acsomega.1c00190
- Pokpas K. Jahed, N., Baker, P. G., & Iwuoha E. I. (2017). Complexation-based detection of nickel(II) at a graphene-chelate probe in the presence of cobalt and zinc by adsorptive stripping voltammetry. *Sensors*, 17(8), 1711. https://doi.org/10.3390/s17081711
- Prathumsuwan T., Jamnongsong S., Sampattavanich S., & Paoprasert P. (2018). Preparation of carbon dots from succinic acid and glycerol as ferrous ion and hydrogen peroxide dual-mode sensors and for cell imaging. *Optical Materials*, 86, 517-529. https://doi.org/10.1016/j.optmat.2018.10.054.
- Quarles C. D., Jones D. R., Jarrett J. M., Shakirova G., Pan Y., Caldwell K L., & Jones R. L. (2014). Analytical method for total chromium and nickel in urine using an inductively coupled plasma-universal cell technology-mass spectrometer (ICP-UCT-MS) in kinetic energy discrimination (KED) mode. *Journal of Analytical Atomic Spectrometry*, 29(2), 297. https://doi.org/10.1039/c3ja50272d
- Rao L., Tang Y., Lu H., Yu S., Ding X., Xu K., Li Z., & Zhang J. Z. (2018). Highly photoluminescent and stable N-doped carbon dots as nanoprobes for Hg<sup>2+</sup> detection. *Nanomaterials*, 8(11, 900. https://doi.org/10.3390%2Fnano 8110900
- Redondo-Fernandez G., Canga J.C., Soldado A., & Encinar J.R. (2023). Functionalized heteroatom-doped carbon dots for biomedical applications: a review. *Analytica Chimica Acta*, 1284, 341874. https://doi.org/ 10.1016/j.aca.2023. 341874.

- Rekhi R., Kaur R., Rani S., Malik A. K., Kabir A., Kenneth G., & Furton K. G. (2016). Determination of cobalt (II), nickel (II) and palladium (II) ions via fabric phase sorptive extraction combination with in performance liquid chromatography-UV detection. Separation Science and Technology. 52(1), 81-90. https://doi.org/10.1080/ 01496395.2016.1232273
- Sadhanala H. K., Aryal S., Sharma K., Orpaz Z., Michaeli S., & Gedanken A. (2022). Nitrogen doped carbon dots as a highly selective and sensitive fluorescent probe for sensing Mg<sup>2+</sup> ions in aqueous solution, and their application in the detection and imaging of intracellular Mg<sup>2+</sup>. Sensors and Actuators B: Chemical, 366, 131958. https://doi.org/10.1016/j.snb.2022. 131958
- Schrenk D., Bignami M., Bodin L., Chipman J. K., Mazo J. D., Grasl-Kraupp B., Hogstrand C., Hoogenboom L. R., Leblanc J. C., Nebbia C. S., Ntzani E., Petersen A., Salomon S., Schwerdtle T., Vleminckx C., Wallace H., Guerin T., Massanyi P., Loveren H. V., Baert K., Gergelova P., & Nielsen E. (2020). Update of the risk assessment of nickel in food and drinking water. *EFSA Journal*, 18, 6268. https://doi.org/10.2903/j.efsa.2020.6268
- Shibata H., Abe M., Sato K., Uwai K, Tokuraku K, & limori T. (2022). Microwave-assisted synthesis and formation mechanism of fluorescent carbon dots from starch. *Carbohydrate Polymer Technologies and Applications*, 3, 100218. https://doi.org/10.1016/j.carpta.2022.1002 18
- Sun L., Wei W., Zhang H., Xu J., & Zhao X. (2022). A Simple colorimetric and fluorescent 'on-off-on' dual-mode sensor based on cyan fluorescent carbon dots/AuNPs for the detection of L-cysteine and zinc thiazole. *Microchemical Journal*, 174, 107079. https://doi.org/10.1016/j.microc.2021.107079
- Sun X., Zhang J., Wang X., Zhao J., Pan W., Yu G., Qu Y., & Wang J. (2020). Colorimetric and fluorimetric dual mode detection of Fe<sup>2+</sup> in aqueous solution based on a carbon dots / phenanthroline system. *Arabian Journal of Chemistry*, 13(4), 5075-5083. https://doi.org/ 10.1016/j.arabjc.2020.02.007
- Varisco M., Zufferey D., Ruggi A., Zhang Y., Erni R., & Mamula O. (2017). Synthesis of hydrophilic and hydrophobic carbon quantum dots from waste of wine fermentation. *Royal Society Open Science*, 4, 170900. http://dx.doi.org/10.1098/rsos.170900
- Wang M., Huang H., Wang L., Sun M., Hou H., & Yang X. (2023). Carbon dots-based dualemission proportional fluorescence sensor for ultra-sensitive visual detection of mercury ions in natural water. *Colloids and surfaces A:*

- Physicochemical and Engineering Aspects, 67520, 132080. https://doi.org/10.1016/j.colsurfa.2023.132080.
- Wang L., Choi W. M., Chung J. S., & Hur S. H. (2020).
  Multicolor Emitting N-Doped Carbon Dots derived from ascorbic acid and phenylenediamine precursors. Nanoscale Research Letters, 15(1), 222. https://doi.org/10.1186/s11671-020-03453-3
- Xu J., Wang Y., Sun L., Qi Q., & Zhao X. (2021). Chitosan and K-Carrageenan-Derived Nitrogen and Suphur Co-doped carbon dots 'on-off-on' fluorescent probe for sequential detection of Fe<sup>3+</sup> and ascorbic acid. *International Journal of Biological Macromolecules*, 191(2021), 1221– 1227. https://doi.org/10.1016/j.ijbiomac. 2021.09.165
- Xu J., Qi Q., Sun L., Guo X., Zhang H., & Zhao X. (2022). Green fluorescent carbon dots from chitosan as selective and sensitive 'off-on' probes for nitrite and 'on-off-on' probes for enrofloxacin detection. *Journal of Alloys and Compound*, 908: 164519. https://doi.org/10. 1016/j.jallcom.2022.164519
- Yanyan Z., Lin J., Xie L., Tang H., Wang K., & Liu J. (2021). One-step preparation of nitrogen doped graphene quantum dots with anodic electrochemiluminescence for sensitive detection of hydrogen peroxide and glucose. *Frontiers in Chemistry*, 9(2021), 688358. http://dx.doi.org/10.3389/fchem.2021.688358
- Yao Q., Feng Y., Rong M., He S., & Chen X. (2017).

  Determination of nickel (II) via quenching of the fluorescence of boron nitride quantum dots. *Microchimica Acta*, 184(48), 4217.

  http://dx.doi.org/10.1007/s00604-017-2496-5
- Yao B., Huang H., Liu Y., & Kang Z. 2019. Carbon dots: A Small conundrum. *Trends in Chemistry*, 1(2), 235-246. https://doi.org/10.1016/j.trechm.2019.02.003
- Yin P., Zou T., Yao G., Li S., He Y., Li G., Li D., Tan W., & Yang M. (2023). In situ microwave-assisted preparation of NS-codoped carbon dots stabilized silver nanoparticles as an off-on fluorescent probe for trace Hg<sup>2+</sup> detection. *Chemosphere*, 338, 139451. https://doi.org/10.1016/j.chemosphere.2023.139451
- Yoo D., Park Y., Cheon B., & Park M.H. (2019). Carbon dots as an effective fluorescent sensing platform for metal ion detection. *Nanoscale Research Letters*, 14(1), 272. https://doi.org/10.1186/s11671-019-3088-6.
- Zhang Q., Xie S., Yang Y., Wu Y., Wang X., Wu J., Zhang L., Chen J., & Wang Y. (2018). A Facile synthesis of highly nitrogen doped carbon dots for imaging and detection in biological samples. *Journal of Analytical Methods in Chemistry*, 2018, 1-9. http://dx.doi.org/10.1155/2018/7890937

Zhao Q., Li X., Wang X., Zang Z., Liu H., Li L., Yu X., Yang X., Lu Z., & Zhang X. (2022). Surface amino group modulation of carbon dots with blue, green and red emission as Cu<sup>2+</sup> ion

reversible detector. *Applied Surface Science*, 598, 153892. https://doi.org/10.1016/j.apsusc.2022.153892.